

Provided for non-commercial research and education use.
Not for reproduction, distribution or commercial use.



This article appeared in a journal published by Elsevier. The attached copy is furnished to the author for internal non-commercial research and education use, including for instruction at the authors institution and sharing with colleagues.

Other uses, including reproduction and distribution, or selling or licensing copies, or posting to personal, institutional or third party websites are prohibited.

In most cases authors are permitted to post their version of the article (e.g. in Word or Tex form) to their personal website or institutional repository. Authors requiring further information regarding Elsevier's archiving and manuscript policies are encouraged to visit:

<http://www.elsevier.com/copyright>



Contents lists available at ScienceDirect

Developmental Biology

journal homepage: www.elsevier.com/developmentalbiology

The *Caenorhabditis elegans* Ste20 kinase, GCK-3, is essential for postembryonic developmental timing and regulates meiotic chromosome segregation

Adam P. Kupinski¹, Thomas Müller-Reichert², Christian R. Eckmann*

Max Planck Institute of Molecular Cell Biology and Genetics (MPI-CBG), Pfotenhauerstrasse 108, 01307 Dresden, Germany

ARTICLE INFO

Article history:

Received for publication 1 March 2010

Revised 21 May 2010

Accepted 24 May 2010

Available online 1 June 2010

Keywords:

GCK-3

Ste20 kinase

Larval development

Germ line development

Spermatogenesis

ABSTRACT

Ste20 kinases constitute a large family of serine/threonine kinases with a plethora of biological functions. Members of the GCK-VI subfamily have been identified as important regulators of osmohomeostasis across species functioning upstream of ion channels. Although the expression of the two highly similar mammalian GCK-VI kinases is eminent in a wide variety of tissues, which includes also the testis, their potential roles in development remain elusive. *Caenorhabditis elegans* contains a single ancestral ortholog termed GCK-3. Here, we report a comprehensive analysis of *gck-3* function and demonstrate its requirement for several developmental processes independent of ion homeostasis, i.e., larval progression, vulva, and germ line formation. Consistent with a wide range of *gck-3* function we find that endogenous GCK-3 is expressed ubiquitously. The serine/threonine kinase activity of GCK-3, but not its presumed C-terminal substrate interaction domain, is essential for *gck-3* gene function. Although expressed in female germ cells, we find GCK-3 progressively accumulating during spermatogenesis where it promotes the first meiotic cell division and facilitates faithful chromosome segregation. In particular, we find that different levels of *gck-3* activity appear to be important for various aspects of germ line development. Taken together, our findings suggest that members of the GCK-VI kinase subfamily may act as key regulators of many developmental processes and that this newly described role in meiotic progression might be conserved and an important part of sexual reproduction.

© 2010 Elsevier Inc. All rights reserved.

Introduction

Tissue formation and differentiation are complex processes that are tightly linked and regulated by the organism's developmental program. The orchestration of cell fates, proliferation, differentiation, and cell survival in response to external or internal clues are often achieved by signaling cascades that rely on multiple protein modifications including phosphorylation by protein kinases. This simple chemical reaction is so crucial that the human and *Caenorhabditis elegans* kinome share over 80% of predicted kinases (Manning, 2005), yet most of their roles in the development of an organism are still largely unknown.

The Ste20 group kinases have attracted increasing attention over the past several years due to their expanding physiological roles. Originally named after the yeast serine/threonine kinase Ste20p, involved in filamentation, mating, and osmoregulation, members are

divided into two families according to their domain organization; GCK (germinal center kinases) and PAK (p21-activated kinases) (Dan et al., 2001). The GCK family has been further classified into eight subfamilies containing essentially a single representative each in *C. elegans*. Surprisingly little is known about their roles in development.

Recently, GCK-VI subfamily members have been implicated in regulating osmohomeostasis in mammalian cells and nematodes. Mammalian SPAK and OXSR1 have been predominantly analyzed in tissue culture cells where they physically interact with the cation-chloride cotransporters KCC3, NKCC1, and NKCC2 (Piechotta et al., 2003; Piechotta et al., 2002) and phosphorylate NKCC1 (Dowd and Forbush, 2003; Moriguchi et al., 2005). *C. elegans* GCK-3 was found to interact with and repress the chloride channel CLH-3b in a phosphorylation-dependent manner (Denton et al., 2005; Falin et al., 2009). CLH-3 is the *C. elegans* ortholog of the mammalian CLC2 chloride channel (Rutledge et al., 2001). CLH-3 activity modulates the contractions of sheath cells during ovulation and GCK-3-mediated CLH-3b phosphorylation is predicted to inhibit the CLC anion channel before oocyte meiotic maturation (Falin et al., 2009; Rutledge et al., 2001; Strange et al., 2006). Nevertheless, *clh-3* mutants are fertile. The genetic dependency of *clh-3* activity on *gck-3* was also proposed to regulate renal tube formation in worms (Hisamoto et al., 2008). Thus, the regulation of ion homeostasis emerges as one example of an evolutionary conserved function among GCK-VI kinases (Strange et al., 2006).

* Corresponding author. Fax: +49 351 210 1289.

E-mail address: eckmann@mpi-cbg.de (C.R. Eckmann).¹ Present address: Center for Regenerative Therapies (CRTD), Technical University of Dresden, Tatzberg 47-49, 01307 Dresden, Germany.² Present address: Medizinisch Theoretisches Zentrum (MTZ), Technical University of Dresden, Fiedlerstrasse 42, 01307 Dresden, Germany.

All known GCK-VI members share conserved domain architecture, an N-terminal kinase domain and two putative regulatory regions named PF1 (PASK and Fray) and PF2, located at the C-terminus (Fig. 1A) (Chen et al., 2004; Leiserson et al., 2000). In the case of OXSR1, the PF1 region is crucial for OXSR1 kinase function, whereas the PF2 domain is dispensable (Chen et al., 2004). The PF2 domain, also termed CCT (conserved C-terminal) domain (Vitari et al., 2006), was found in all GCK-VI orthologs to provide a protein interaction platform for the few substrates known (Anselmo et al., 2006; Choe and Strange, 2007; Gagnon et al., 2006b; Moriguchi et al., 2005; Piechotta et al., 2003; Vitari et al., 2006). Strikingly, the only known regulators of GCK-VI kinases also require the PF2 domain for their physical interaction. These proteins are members of the conserved without-lysine kinase (WNK) family and are implicated in osmoregulation and other biological processes (Choe and Strange, 2007; Lee et al., 2004; Moriguchi et al., 2005; Oh et al., 2007; Vitari et al., 2005; Xu et al., 2004; Zagorska et al., 2007). Mammalian GCK-VI and WNK proteins are widely expressed, suggesting that individualized functions with combinatorial actions may occur in many organs (Vitari et al., 2005; Xu et al., 2000). Knockout mice with compromised OXSR1 function are embryonic lethal, whereas SPAK knockout mice are viable and show reduced fertility and mild behavioral defects, suggesting that OXSR1 and SPAK are not fully redundant with each other and specialized functions may exist (Geng et al., 2009). Mice homozygotes for WNK1, one paralog out of four encoded WNK proteins, are also embryonic lethal (Zambrowicz et al., 2003). These drastic phenotypes underscore the importance of GCK-VI and WNK protein family members in the development of an organism; however, their precise functions in vivo remain to be elucidated.

In *C. elegans*, RNAi knockdown experiments of WNK-1 or GCK-3 demonstrated a shared role for both proteins in acute volume recovery and survival after hypertonicity-induced shrinkage (Choe and Strange, 2007). Both genes are also implicated in the formation of the tubular extensions of the excretory cell, which is a part of the animal's renal system, together with associated gland, duct and pore cells (Hisamoto et al., 2008). Although a hypomorphic allele of *gck-3* had been described, the null phenotype and hence the full range of *gck-3* functions during development remained obscure. Unfortunately, confusing data on the *bona fide* promoter of the *gck-3* locus exist and previous promoter-driven GFP expression studies may have left a rather incomplete picture of the expression profile of GCK-3 (Choe and Strange, 2007; Denton et al., 2005).

Here we report novel developmental functions of the worm GCK-VI kinase, GCK-3, by analyzing the first genetic and molecular null allele. We find that GCK-3 kinase activity promotes larval progression beyond the L2 stage and coordinates developmental timing of postembryonic organ development. Most somatic defects affect a broad spectrum of developmental decisions that appear independent of its role in ion homeostasis. We find GCK-3 expression upregulated in spermatogenesis and its function is crucial for male meiosis. We demonstrate that a reduction or a complete loss of *gck-3* activity results in meiotic chromosome segregation defects or metaphase I arrested spermatocytes, respectively. Furthermore, in the most severe cases, meiosis and gametogenesis are altogether abolished. These novel meiosis defects may also represent a conserved function of GCK-3 in sexually reproducing animals as mammalian GCK-VI members are highly expressed in testis.

Material and methods

Strains

Worm strains are derivatives of the wild-type Bristol strain N2 and were maintained at 20 °C as described (Brenner, 1974). The *gck-3(q733)* LG V allele was isolated in a PCR-based screen for deletion mutants induced by EMS and backcrossed nine times (Kraemer et al., 1999). The

outer and inner primer pairs used for screening were OutFwd GTTGAGTGAAGTATCGGAC; OutRev GTCTCGATACTCACCACCTT and InFwd CAGAGTCTCATACTGTTGTTG; InRev AATCACGGCTCACTTCGTG.

One-on-one mating tests were performed with *fog-2(RNAi)* feminized hermaphrodites and males from EV285 mothers. Adult animals were staged as 24–36 hours past the mid L4 stage. Primers for genotyping are available upon request. The following strains were used:

EV11 *gck-3(q733)/dpy-21(e428) unc-80(e1272) V*
 EV232 *gck-3(tm1296)/dpy-21(e428) V*
 EV285 *him-8(e1489) IV; gck-3(tm1296)/dpy-21(e428) V*
 TY832 *yDf4/dpy-11(e224) unc-76(e911) V*
 EV141 *gck-3(q733)/unc-76(e911) V; evEx1[unc-122::GFP; let-858::GFP; gck-3(WT-cDNA)]*
 EV190 *gck-3(q733)/unc-76(e911) V; evEx2[unc-122::GFP; let-858::GFP; gck-3(K137R-cDNA)]*
 EV236 *gck-3(q733)/unc-76(e911) V; evEx6[unc-122::GFP; aqp-8::GFP; gck-3(WT-cDNA)]*
 EV235 *gck-3(q733)/unc-76(e911) V; evEx5[unc-122::GFP; dpy-7::GFP; gck-3(WT-cDNA)]*
 AA86 *daf-12(rh61rh411) X*
 GR1348 *pha-1(e2123) III; mgEx646[mlt-10p::gfp-pest pha-1]*

DNA constructs

The *gck-3* ORF encoding aa 2–596 was subcloned into pCITE-4a (Novagen) from an RT-PCR product with appropriate primers. The GCK-3^{K137R} mutant was created using QuikChange (Stratagene). GCK^{WT} and GCK^{K137R} cDNAs were cloned in frame downstream of GFP of a pELT vector, which is a derivative of the pPD118.25 plasmid (Fire lab vector kit) containing an N-terminal GFP fusion cassette under the control of the *let-858* promoter and 3'UTR. *let-858* promoter was replaced with *aqp-8* (Mah et al., 2007) or *dpy-7* (Gilleard et al., 1997) promoter in pELT GFP::GCK-3.

Transgenic lines

EV11 animals were injected with a DNA mixture containing a pELT construct and the transformation marker *unc-122::GFP* at a dilution of 2–10 ng/μl and 90 ng/μl, respectively. Transgenic progeny was visually inspected for GFP expression in coelomocytes and for ubiquitous GCK-3 expression. *aqp-8* and *dpy-7* promoter pELT constructs were injected without a transformation marker.

Antibody generation

A GST fusion of C-terminal GCK-3 fragment (aa 388–596) was affinity purified from BL21 *Escherichia coli* cells and injected into two rats after SDS gel purification. After initial tests, the serum of rat #3 was affinity purified against an identical GCK-3 His-tagged fragment immobilized on an NHS column (Amersham). Immunoblots were generated with preblocked antibodies against *E. coli* (OP50) acetone powder (Miller and Shakes, 1995).

Western blotting analysis

For total worm extracts, 20 hermaphrodites and 40 males were single picked and immediately frozen in liquid nitrogen. After resuspension in SDS sample buffer, samples were sonicated in a water bath for 10 minutes and boiled for 5 min before SDS-PAGE separation. The gonads from 30 hermaphrodites and 50 males were extruded in a glass Petri dish in M9 solution containing 0.25 mM levamisole and 0.02% Triton X-100. The carcass was removed with a sharp needle, and the individual gonadal arms were transferred in batches of ten to a tube and immediately frozen in liquid nitrogen. Samples were resolved by SDS-PAGE and probed by immunoblotting

with anti-GCK-3 (1:1000) and anti-tubulin (clone B-5-1-2, Sigma) antibody. The mean intensity of bands was quantified using the histogram function of Photoshop CS3 (Adobe).

Immunocytochemistry

Immunostainings with methanol fixation (Figs. 3 and 4) or 1% PFA (Figs. 6 and 7) were performed as described (Crittenden and Kimble, 1999). Secondary antibodies (Jackson Laboratories) were coupled to fluorochromes FITC, CY3, and CY5, and specimens were stained with DAPI (10 ng/ml) before their embedding in VectaShield (VectaLabs). Images were taken on a Zeiss Imager Z1 equipped with an AxioCam MRm (Zeiss) and processed with AxioVision (Zeiss) and Photoshop CS3 (Adobe). Optical sections were taken with an Apotome (Zeiss) and maximum intensity projections (Figs. 4 and 7) were generated with the Axiovision software (Zeiss).

High-pressure freezing and transmission electron microscopy (TEM)

Whole worms were cryoimmobilized using an EM PACT2 + RTS high-pressure freezer (Leica Microsystems; McDonald et al., 2007). Samples were freeze-substituted at -90°C for 42 h in acetone containing 1% osmium tetroxide and 0.1% uranyl acetate (Muller-Reichert et al., 2003). The temperature was raised progressively to room temperature over 22 h in an automatic freeze-substitution machine (Leica EM AFS). Samples were thin-layer embedded in Epon/Araldite, and thin sections (70 nm) were cut using a Leica Ultracut UCT microtome aiming for the central region of the animal; no pharyngeal or anal structures were present in the images. Sections were collected on Formvar-coated copper grids, poststained with 2% uranyl acetate in 70% methanol followed by aqueous lead citrate and viewed in a TECNAI 12 (FEI) transmission electron microscope operated at 100 kV. Quantifications in Fig. 4 and Supplementary Fig. 3 were done using Image J.

GCK-3 kinase assay

N-terminal GST fusion proteins of GCK-3^{WT} and GCK-3^{K137R} were expressed in BL21 *E. coli* and bound to glutathione beads. GCK-3 proteins were released from their GST moiety by overnight incubation with PreScission protease (Roche) at 4 °C. Kinase assays were performed as described in Johnston et al. (2000). In parallel, an assay with cold ATP was performed for mass spectrometric analysis.

Mass spectrometric (MS) analysis

The Coomassie-visualized GCK-3 band was excised from SDS-PAGE gels followed by in-gel digestions with various proteases and/or their combinations in independent experiments; for GluC and ArgC digestion, see the manufacturer's protocols (Roche), and for trypsin, see Shevchenko et al. (2006). To produce peptides detectable by mass spectrometry from Lys-rich stretches in the protein sequence, amino groups of lysines were in-gel propionylated before the digestion (Peters et al., 2003). After digestion, peptides were extracted twice with 50 μl of 5% formic acid and 50% acetonitrile, dried in a vacuum centrifuge and redissolved in 20 μl of 5% (vol./vol.) formic acid for LC-MS/MS analysis on an Ultimate 3000 nanoLC system (Dionex, Amsterdam) interfaced on-line to a LTQ Orbitrap hybrid mass spectrometer (Thermo Fisher Scientific) via a robotic nanoflow ion source TriVersa (Advion BioSciences Ltd., Ithaca, NY) as described in Junqueira et al. (2008) using 3.5 h gradient of 5% to 60% of acetonitrile in 0.1% formic acid. Acquired MS/MS spectra were determined by NCBI protein sequences database searches or individual protein sequences using MASCOT software (Matrix Science, v.2.2.0); the mass tolerance was set to 20 ppm for peptide masses and 0.5 Da for masses of peptide fragments; variable modification: propionamide

(C), carbamydomethyl (C), *N*-acetylation (protein N-terminus), oxidation (M); propionyl (K); enzyme: no enzyme specificity; one missed cleavage was allowed. All peptide matches with peptide ions score above 25 were manually evaluated.

Results

gck-3 is a downstream gene in an operon and encodes a broadly expressed protein kinase

To study the role of certain protein kinase superfamilies in germ line development, we performed a dsRNAi injection screen and identified a Ste20-related protein encoded by the *gck-3* locus as a putative candidate. Upon knockdown, we observed a very small fraction of sterile adult progeny (<6%, $n=635$) that contained occasionally highly underdeveloped germ lines (data not shown). During our studies, *gck-3* was reported as an SL1 spliced mRNA from a single locus gene (Denton et al., 2005). However, our transcript analysis indicates that *gck-3* is a downstream gene in a syntenic operon with the uncharacterized gene Y59A8B.22 in three related nematode species (Supplementary Fig 1A). This strongly suggests that the endogenous promoter of *gck-3* is most likely rather complex, which is consistent with a more recent study (Choe and Strange, 2007). Furthermore, due to the large region covered by this operon (>30 kb), its sequence elements will be difficult to identify without knowing the true expression pattern of endogenous GCK-3 protein.

As indicated, RNAi knockdowns of *gck-3* were difficult to reproduce; the injection of dsRNA produced strong phenotypes at a very low frequency (<2%, $n>500$) and feeding dsRNA to the worms resulted in very weak or no phenotypes (data not shown). To avoid complications by using RNAi-sensitized backgrounds, we isolated a *gck-3* deletion mutant in a reverse genetic mutagenesis screen and recovered the *gck-3(q733)* allele. Its genome misses 898 nucleotides, affecting the entire second exon and flanking intronic sequences, which leads to a frame shift in the ORF of the *gck-3(q733)* mRNA, as confirmed by RT-PCR and cDNA sequencing (Supplementary Fig. 1A). The remaining GCK-3 polypeptide comprises the nonconserved amino terminus lacking any obvious functional domains (Fig. 1A). In a genetic test with the chromosomal deficiency *yDf4*, we observed no obvious phenotypic difference between *gck-3(q733)* homozygotes and *gck-3(q733)/yDf4* trans-heterozygotes (data not shown). Recently, a hypomorphic *gck-3(tm1296)* mutation that deletes the PF2 domain in the C-terminus was reported (Fig. 1A) (Hisamoto et al., 2008). Homozygote *gck-3(tm1296)* animals were much less affected in their development than *gck-3(q733)* homozygotes (see below). To test the strength of either mutation, we generated *gck-3(q733)/gck-3(tm1296)* trans-heterozygotes and observed a phenotype similar to *gck-3(q733)* homozygotes (data not shown). Taken together, our genetic analysis suggests that the *gck-3(tm1296)* allele is a loss-of-function allele of *gck-3*, retaining some *gck-3* activity, and that the *gck-3(q733)* allele is a true genetic null allele, hereafter referred to as *gck-3(q733)*.

To address GCK-3 expression profiles, we generated affinity-purified polyclonal anti-GCK-3 antibodies. A single protein of approximately 70 kDa (predicted MW of 64 kDa), absent in *gck-3(q733)* animals, was detected in extracts of staged animals (Fig. 1B, see also Fig. 6F). GCK-3 is expressed continuously during worm development from embryogenesis to adulthood. Unfortunately, our C-terminal anti-GCK-3 antibodies did not cross react with the truncated form of the *tm1296*-encoded polypeptide, preventing us from assessing how much GCK-3 is still produced in *gck-3(tm1296)* animals (Fig. 1B and Supplementary Figs. 1B and C).

Previous data on GCK-3 kinase activity was limited to unpurified fusion proteins, expressed in heterologous systems, which also contained orthologous genes of this evolutionary conserved protein (Denton et al., 2005; Hisamoto et al., 2008). To verify that GCK-3 is a

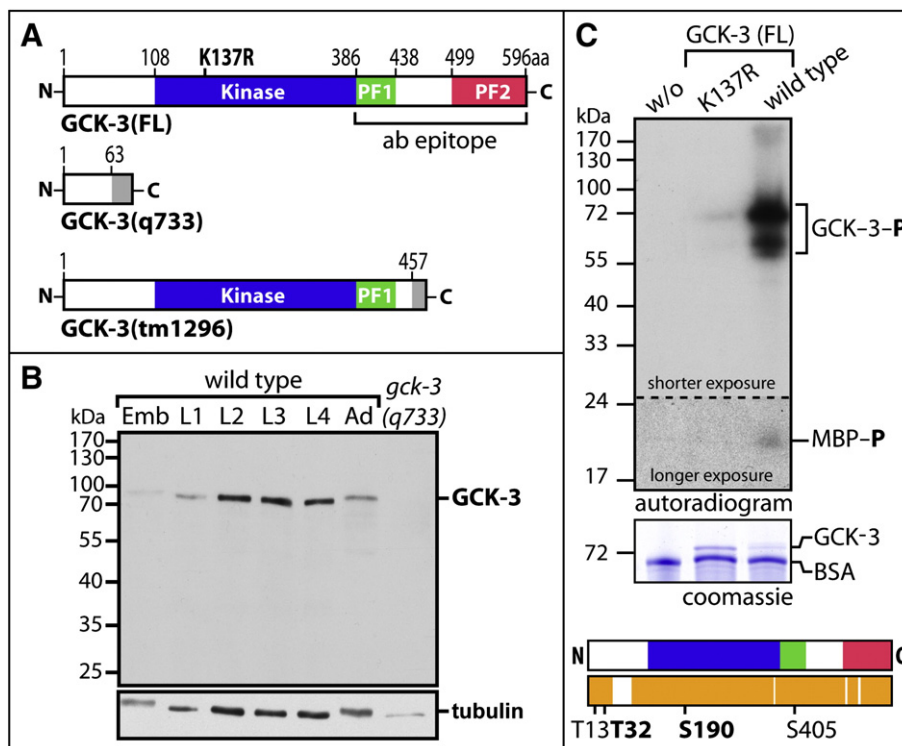


Fig. 1. GCK-3 expression and kinase activity. (A) Protein domain organization of full-length (FL) GCK-3 and putative GCK-3 truncations in given mutants. Novel amino acids are in grey, and the fragment used for antibody generation (ab) is indicated. (B) GCK-3 developmental expression profile. Emb, embryos; L1–4, larval stages; Ad, adult. (C) Recombinant GCK-3 kinase activity. (top) Wild-type and kinase-inactive (K137R) GCK-3 assayed for autophosphorylation or with the artificial substrate myeline basic protein (MBP) on the same protein gel. Lane marked w/o contains no GCK-3. (bottom) LC-MS/MS mapped autophosphorylation sites with predominantly modified residues in bold. Domain colors according to (A); orange, sequence coverage.

serine/threonine protein kinase by itself, we performed a kinase assay using recombinant GCK-3 (highly pure and untagged) and myelin basic protein (MBP) as an artificial substrate (Fig. 1C). As a negative control, we mutated lysine 137 within the kinase domain to an arginine, generating the GCK-3^{KR} mutant (Fig. 1A). We observed a weak but specific phosphorylation activity of GCK-3^{WT} on MBP. We also discovered a strong autophosphorylation activity of GCK-3^{WT} that depends entirely on its active kinase domain (Fig. 1C). For both substrates, the GCK-3^{KR} mutation abolished kinase activity as predicted (Fig. 1C). To assess which amino acids serve as phosphoacceptor sites for autophosphorylation, we used mass spectrometric analysis and found that Thr32 and Ser190 were strongly phosphorylated, whereas Thr13 and Ser405 were weakly phosphorylated (Fig. 1C). None of the 15 tyrosines was found phosphorylated, suggesting that GCK-3 is a serine/threonine protein kinase.

Zygotic *gck-3* is required for larval development and the molting cycle

To investigate developmental roles of *gck-3*, we focused our analysis on homozygote *gck-3(q733)* deletion mutants derived from heterozygote mothers. In contrast to their adult heterozygote siblings, all *gck-3(q733)* hermaphrodites ($n = 137$) have, at low magnification, a severely reduced body size and are paler, suggesting an early larval arrest (Fig. 2A).

To assess the developmental stage of arrested *gck-3(q733)* animals, we followed their molting by taking advantage of the *mlt-10p::GFP-pest* fluorescent reporter. The reporter is expressed a few hours before shedding of the cuticle and then rapidly degraded (Frandsen et al., 2005). All *gck-3(q733)* animals tested ($n = 10$) showed only one peak of GFP-expression, which contrasts to wild type, where four peaks were observed during the same time period, corresponding to four molts from L1 to adulthood ($n = 10$) (Fig. 2B). Also, the timing of the single molting event was noticeably delayed compared to wild

type (Fig. 2B). We conclude that *gck-3(q733)* animals undergo only one molting event.

In wild-type animals, the cuticle forms lateral ridges that span the length of the animal in the L1 larvae, the dauer stage and in the adulthood, but not in L2–L4 larval stages (Figs. 2C–E). Therefore, we confirmed the larval arrest by examining the morphological appearance of the cuticle by electron microscopy. The arrested *gck-3(q733)* animals examined ($n = 6$) did not form ridges (Fig. 2F), which is consistent with a single molt event and argues also against the dauer stage. Another line of evidence that the phenotype is not an unrecognized dauer arrest is that *gck-3(q733);daf-12(rh61r411)* double mutants remained small-sized and L2-like arrested ($n = 15$). *daf-12* is the most downstream gene in the dauer pathway, and *daf-12(rh61r411)* is able to suppress known dauer constitutive mutations (Riddle et al., 1981).

To exclude the possibility of an aberrant *mlt-10p::GFP-pest* expression in the *gck-3(q733)* background, we followed their successive moltings and counted the number of shed cuticles on the plate. To this end, we transferred L1 synchronized progeny of heterozygote mothers on single plates and monitored their development in regular intervals until the small *gck-3* homozygote mutant animals had died. In addition, we also inspected several small animals at higher magnifications via Nomarski microscopy and compared them to similarly aged heterozygote or non-*gck-3* mutant siblings.

Surprisingly, we found two kinds of similarly small-sized animals that only appeared to have had molted once and lived up to 6 days, compared to 30 days of a continuously developing “wild-type” counterpart (Fig. 2G). The majority of *gck-3(q733)* animals (87.5%, $n = 16$) superficially appeared as L2-like larvae with no fully formed vulva or gametes (Supplementary Fig. 2E). However, a minor class of *gck-3(q733)* animals (12.5%, $n = 16$) had developed an everted vulvae and possessed an adult-type alae (Supplementary Figs. 2B, C, and I).

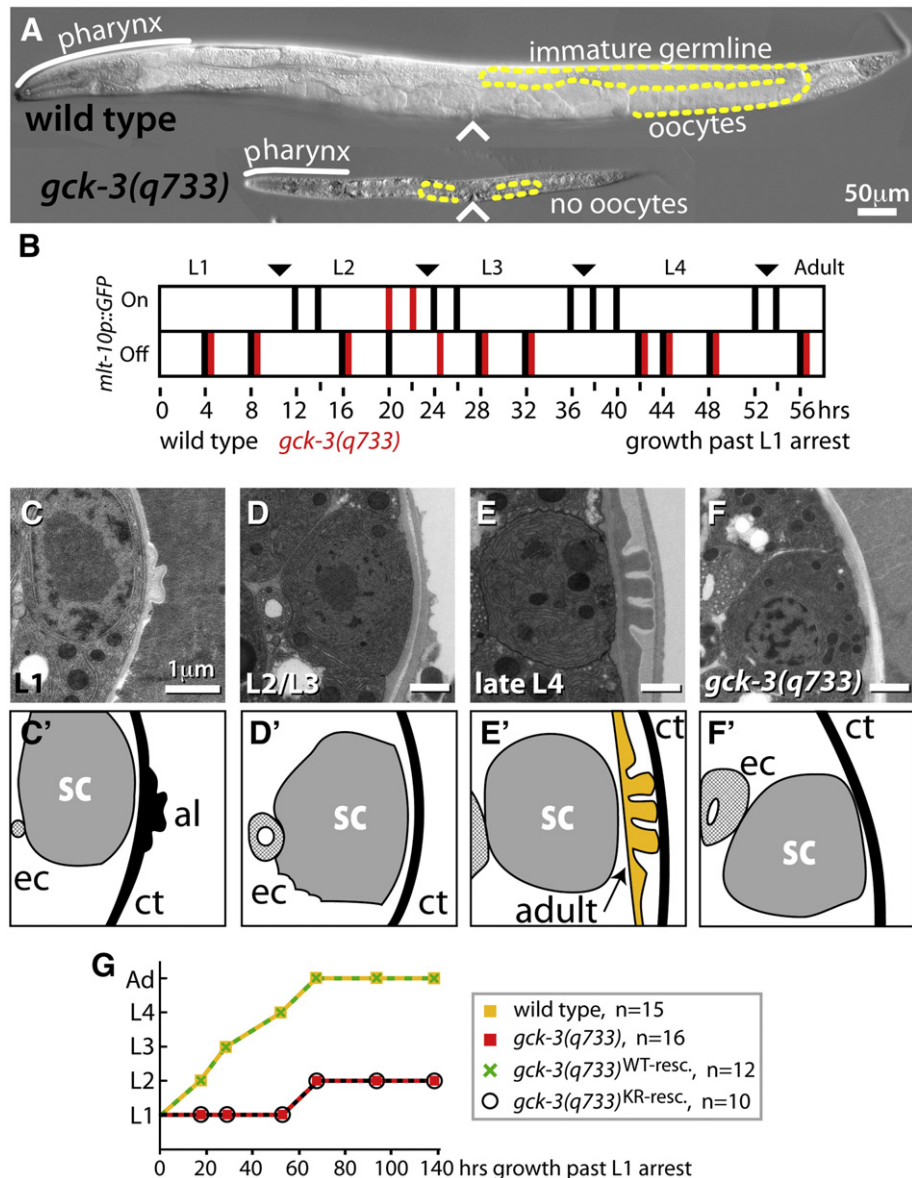


Fig. 2. *gck-3(q733)* larval arrest. (A) Nomarski images of similarly aged wild-type and *gck-3(q733)* animals. Yellow dashed line, outline of the germ line; white caret, position of the vulva. (B) Graph of *mlt-10p::GFP* expression. Individual molting events were followed after L1 synchrony. (C–F') TEM images of wild-type larvae and *gck-3(q733)* animals in cross-sections. ec—excretory cell, sc—seam cell, ct—cuticle, al—alae, adult—adult alae. (G) Molting graph of indicated genotypes derived from monitoring the animals at the given time points and counting shed cuticles. Arrested *gck-3(q733)* animals died around 140 h, whereas adult animals continued to live longer (not shown).

These animals were sterile, containing a highly underproliferated germ line and lacked differentiated gametes, yet had no overt abnormalities in the somatic parts of the gonad (Supplementary Fig. 2D). Strangely, we were not able to catch multiple molting events nor did we recover more than one shed cuticle, suggesting that we either had not identified all cuticles/molts or that the animals started to secrete the alae structure independently of completing multiple molt cycles. The former possibility gains support by the fact that these cuticles are extremely small and hard to detect; however, we would have to have missed three additional cuticles/molts, which is unlikely. In support of the latter hypothesis is our molting reporter analysis, where we did not observe more than one expression peak of the molting reporter. Therefore, we propose that these animals undergo an alternative second molting cycle that may be more adult-like. In summary, we conclude that the loss of *gck-3* activity results in two classes of small-sized animals that have a similar molting behavior from the L1 stage to the L2 stage but differ in the morphology of the cuticle and the developmental stage of the vulva. The larger fraction

arrest as L2-like animals and the small fraction appears small adult-like with vulva and germ line formation defects.

gck-3 is required for coordinated postembryonic development

Next, we analyzed the overall developmental defects of the L2-like arrested animals in more detail by assessing the developmental status of two internal organs that depend postembryonically on the developmental age of the animal, i.e., the vulva and the gonad. The status of these organs is often used to gauge the developmental stage of the animal. To visualize the global organization of the tissues, we stained fixed animals with the chromatin dye DAPI (Fig. 3). In wild-type animals, gonadogenesis and vulva formation are linked, with timing correlated to larval progression (Kimble and Hirsh, 1979; Sulston and Horvitz, 1977). In the L2 stage, the germ cells are in the center of the developing gonad, and only the vulval precursor cells are specified (Figs. 3A and B). In early L3, the gonadal primordium rearranges to form a central somatic structure flanked by two

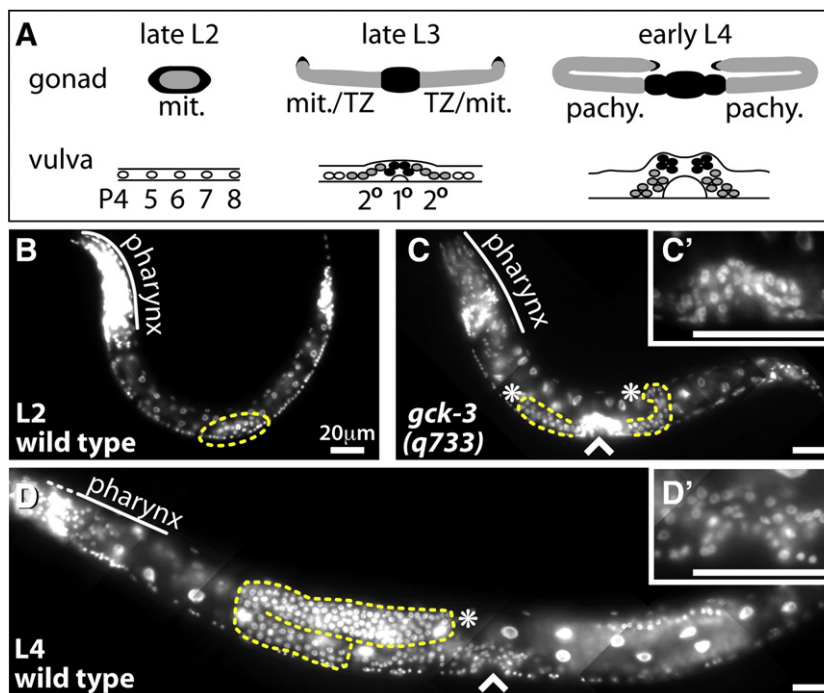


Fig. 3. *gck-3* is required for coordinated postembryonic development. (A) Scheme of correlated gonad and vulva development. Somatic gonadal cells in black and germ cells in grey: mit.—mitosis, TZ—transition zone, pachy.—pachytene. In L3 and L4, only the two somatic distal tip cells, which cap the two germ line arms, and central uterine/spermatheca cells are depicted for simplicity. Uninduced vulva precursor (P) cells give rise to primary (1°) and secondary (2°) vulva fates. (B–D') Nuclei visualized by DAPI staining. Yellow dashed line, outline of the germ line; white caret, position of the vulva; asterisk, distal tip cell location. (B) Wild-type L2 larvae have an immature gonad and no vulva. (C) L2-like arrested *gck-3* (*q733*) animal, which is of similar age to an adult hermaphrodite. Take notice of two small germ line arms and a vulva similar to a (D) wild-type L4 larvae. (C' and D') Magnified vulva arch.

outgrowing gonadal arms that contain proliferating germ cells (Fig. 3A). The vulval cell fate is induced by the gonadal anchor cell, and vulva formation becomes morphologically apparent in late L3, resulting in the genesis of a vulval arch in mid-L4 animals (Figs. 3A and D'). Adults possess an everted, highly symmetric vulva (Supplementary Fig. 2F). Concomitant with vulva formation, both germ line arms grow into a U-shaped tube, and the most proximal germ cells enter meiosis in L3 and start differentiating into sperm in L4, while the adult produces oocytes only (Figs. 3A and D).

To our surprise, we find that when heterozygote siblings reached adulthood, L2-like *gck-3*(*q733*) animals displayed defects in gonad and vulva development that do not correlate with their presumed developmental stage. We find that gonadogenesis had proceeded to an L3-like stage with a central somatic gonadal structure and two flanking, small germ line arms (Fig. 3C and Supplementary Fig. 2E). The number of germ cells was similar to that of wild type of the early L3 stage, containing on average ~46 germ cells ($n = 8$). However, no clear meiotic stages were detectable, and gametogenesis was absent. In contrast, vulva formation had initiated and proceeded to form a full arch similar to wild-type L4 animals (Figs. 3C and C'). Nevertheless, none of these organs reaches adult morphologies, which is consistent with a larval-like arrest. Taken together, *gck-3* is required in multiple organs to couple morphogenesis to the developmental stage of the animal. In particular, vulva development and gonad/germ line development are out of synchrony and fail to develop into adult structures.

GCK-3 is expressed in the excretory cell and regulates its growth

Previous transcriptional reporter studies suggested that *gck-3* might be expressed in the excretory cell (Choe and Strange, 2007; Denton et al., 2005). The excretory cell is a large, H-shaped cell that extends laterally throughout the entire animal body and functions as the renal system of the worm (Nelson and Riddle, 1984). To address

the endogenous protein expression pattern of GCK-3, we performed whole-mount immunostainings (Fig. 4). We observed an essentially ubiquitous, low-level anti-GCK-3 staining in most tissues with a pronounced appearance in the excretory cell of the wild type; no staining above background was present in *gck-3*(*q733*) animals (Figs. 4A–C). Subcellularly, GCK-3 is present in the cytoplasm of the excretory cell as compared to the ERM-1, which outlines the canal lumen as an apical membrane-localized protein (Fig. 4A) (Gobel et al., 2004). In addition, the excretory cell body contains increased cytoplasmic levels of GCK-3, which is in contrast to VHA-8, a cytosolic subunit of a vacuolar-type H⁺-ATPase that is almost exclusively localized to the excretory canals (Figs. 4D, E, and F) (Choi et al., 2003).

A previous study reported shortened excretory canals in *gck-3* (RNAi)-treated wild-type or hypomorphic *gck-3*(*tm1296*) animals (Hisamoto et al., 2008). Consistent with this, we find that *gck-3*(*q733*) animals possess also shortened excretory canals (Fig. 4B). However, no animals ($n > 50$) were observed without canals, indicating that *gck-3* is not essential for the formation of the excretory cell. With respect to the excretory cell, both alleles of *gck-3*, the complete and partial loss-of-function allele, show the same phenotype. Furthermore, we compared excretory canal formation among different stages of wild-type to *gck-3*(*q733*) arrested animals by analyzing the ultrastructure of the excretory canal using electron microscopy. In cross-sections of wild-type excretory cells, we observed a circular lumen in the center of the canal surrounded by secretory vesicles (Figs. 4G, H, and I). In parallel to the different larval stages and the increase of body size during development, the excretory cell area and the number of vesicles increased in wild type, ranging from 0.92 mm² and 15 vesicles in L1 stage to 2.86 mm² and 58 vesicles in the L4 stage (Fig. 4M). Although *gck-3*(*q733*) mutant animals do not show gross abnormalities in canal morphology (Figs. 4J and L), we find that the excretory cell of *gck-3*(*q733*) animals resembles that of the L4 wild-type stage with an average of 51 vesicles and 2.4 mm² cell area (Fig. 4M). Occasionally, we observed the formation of additional smaller lumen

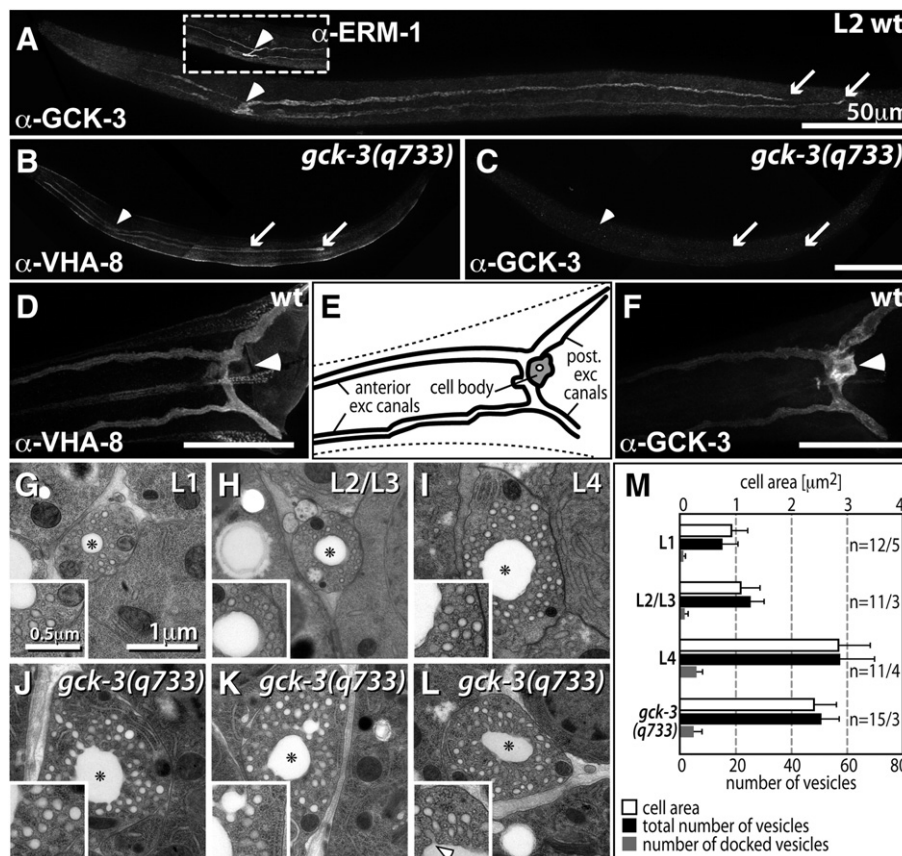


Fig. 4. GCK-3 is expressed in the excretory cell and affects its morphology. (A–F) Images of whole mount immunostained hermaphrodites. (A–C) Entire adult animal or (D and F) a head region fragment. Arrowhead, excretory cell body; arrows, excretory canals posterior tips. (E) Schematic representation of excretory cell structures as in panels D and F. (G–L) TEM images showing posterior excretory canal cross sections. Asterisk, canal lumen. Insets, higher magnification of excretory vesicles. Arrowhead, example of a docked vesicle. (G–I) Wild-type, the animals of the L2/L3 stage were not precisely separated by age. (J–L) Three independent *gck-3(q733)* animals are depicted. (M) Quantification of cell area (top axis) and number of vesicles (bottom axis) in given wild-type larvae and *gck-3(q733)* animals. *n* = number of images/number of animals.

(Fig. 4K) or a complete lack of the entire lumen in cell cross-sections (data not shown). In summary, we conclude that endogenous GCK-3 is expressed in the excretory cell and preferentially enriches in the cytosol. Minor morphological excretory cell defects are present in *gck-3(q733)* animals, such as an enlarged canal in L2-arrested animals and a posterior shortening of the canals. However, no gross morphological abnormalities are eminent.

gck-3 deficient animals show defects in the digestive tract

Another place of GCK-3 expression has been proposed to be the gut for which a physiological function of *gck-3* was suggested (Choe and Strange, 2007). However, we observed several morphological alterations that appear inconsistent with a sole role of GCK-3 in ion homeostasis (Supplementary Fig. 3). Upon feeding GFP-expressing *E. coli*, we observed a striking accumulation of GFP-positive bacteria in the gut lumen in the *gck-3(q733)* arrested animals but not in the wild type (Supplementary Figs. 3A and C). Indeed, intact bacteria are present in the gut of the mutant animals as judged by electron microscopy (Supplementary Fig. 3J). Furthermore, we find that the intestinal lumen is dilated and extensively folded. In single cross sections, we noted more than one intestine lumen, indicating a strong folding of the intestinal lumen that is absent in the wild type (for an example, compare Supplementary Fig. 3E with F). A closer examination of the length of the microvilli revealed that *gck-3(q733)* animals are comparable to wild-type L2 larvae (Supplementary Figs. 3G and M). Furthermore, we confirmed that endogenous GCK-3 is expressed in all gut cells where it localizes to the cytoplasm and to a large extent to the nucleus (data not shown, for an example,

compare Supplementary Figs. 3O and Q). In summary, GCK-3 is expressed in the gut and its absence appears to affect the function of the gut, which fills with undigested bacteria.

Full rescue of the *gck-3(q733)* phenotype requires ubiquitously expressed kinase activity

To investigate if the *gck-3(q733)* phenotypes are caused by a loss of kinase activity or the removal of the protein, we performed somatic rescue experiments. We generated transgenic *gck-3(q733)* animals expressing GFP-tagged GCK-3 under the control of the *let-858* promoter, which is ubiquitously active at a basal level. The *let-858* promoter was chosen because it is often effectively silenced in the germ line as part of extrachromosomal arrays (Kelly et al., 1997) and the endogenous promoter of the extremely large *gck-3* operon was unclear. Several independent lines were obtained and characterized as fully rescued in their soma (Fig. 5). GCK-3^{WT} transgenic animals developed into adulthood in the proper time frame and were essentially indistinguishable from wild-type counterparts (Figs. 5A, B, and C and Fig. 2G). However, these adult hermaphrodites are sterile and produce essentially no embryos; the few embryos produced (on average, 2; *n* = 56) do not develop into living progeny (see below). The GFP::GCK-3^{WT} fusion expressed close to wild-type levels throughout the body of the animal, including somatic cells of the gonad (Fig. 5K, data not shown). Most prominently, GFP::GCK-3^{WT} was enriched in intestinal cells, consistent with endogenous expression as observed by antibody staining (Fig. 5C and Supplementary Fig. 3O). No visible expression of GFP::GCK-3^{WT} was detected in germ cells when probing with either anti-GCK-3 (data not shown; for an

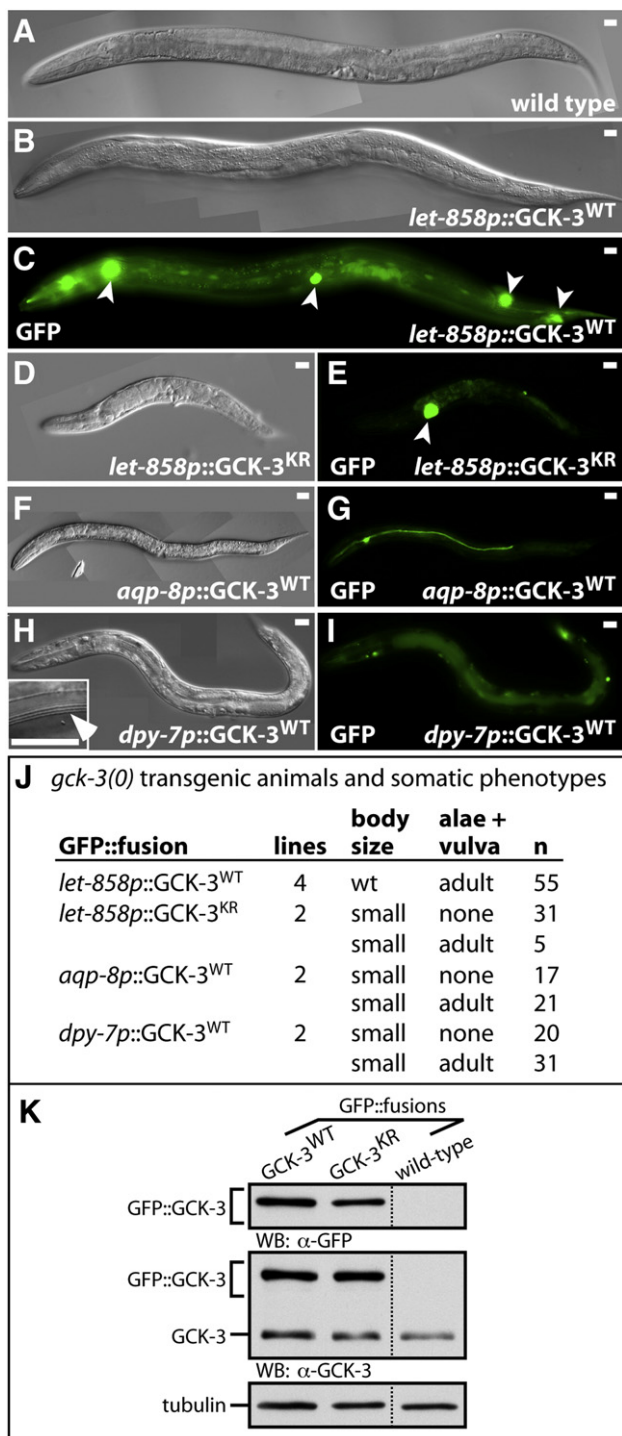


Fig. 5. Somatic rescue of *gck-3(q733)* animals. (A, B, D, F, and H) Nomarski and corresponding (C, E, G, and I) GFP channel images of a wild-type animal or transgenic *gck-3(q733)* hermaphrodites expressing either wild-type or kinase inactive GFP::GCK-3 from given promoters with a mainly (A–E) ubiquitous, (F and G) excretory cell, or (H and I) hypodermal activity. Scale bar, 20 μm. (C and E) White arrowheads, coinjection marker expressed in coelomocytes. (H) Inset, magnified adult alae. (J) Summary of all injected constructs and their ability to rescue the somatic defects of *gck-3(q733)* animals. (K) Immunoblots of worm extracts from *gck-3* heterozygotes carrying the indicated GFP::fusion proteins.

example, see Fig. 6C”) or anti-GFP antibodies (data not shown). To determine whether the kinase activity is essential for all *gck-3* somatic functions, we attempted to rescue *gck-3(q733)* animals with the kinase-dead mutant, GCK-3^{KR}. No rescue of the L2-like or small adult-like phenotype was observed although the fusion protein was

expressed well (Figs. 5D, E, J, and K and Supplementary Fig. 2J). Also, the penetrance of both phenotypic classes was similar to nontransgenic *gck-3(q733)* homozygotes. Transgenic GCK-3^{KR} small adult-like arrested animals occurred with a frequency of 14% ($n = 36$) compared to 12% ($n = 16$) of *gck-3(q733)* homozygotes without a transgene. We conclude that the observed somatic developmental defects in *gck-3(q733)* animals are solely dependent on *gck-3* activity and requires a functional kinase domain.

GCK-3 expression in specific organs does not rescue gck-3(q733) animals

As we observed abundant expression of GCK-3 in the excretory cell (Fig. 4A) we tested if a lack of GCK-3 activity in this cell type is responsible for the developmental defects in *gck-3(q733)* animals. We generated transgenic *gck-3(q733)* animals that expressed GFP::GCK-3^{WT} under the control of the *aqp-8* promoter, which is reported to act exclusively in the excretory cell (Mah et al., 2007). In contrast to a ubiquitous expression of GCK-3, no general rescue was observed, although occasionally the canal-shortening defect was rescued. However, we observed that the penetrance of both classes of *gck-3(q733)* arrested phenotypes had changed. The majority of the small-sized transgenic animals (55%, $n = 38$) showed an adult-type alae and an everted vulva (Figs. 5F, G, and J and Supplementary Fig. 4), and the germ line was strongly underdeveloped and poorly differentiated, similar to the small adult-like *gck-3(q733)* animals (Supplementary Fig. 4A). Fewer transgenic animals (45%, $n = 38$) were L2-like arrested, suggesting that the number of small adult-like animals is increased, therefore, representing a partial rescue of the prevailing *gck-3(q733)* L2-like arrest (Fig. 5J). In any case, no rescue to adulthood as seen with the ubiquitous *let-858* promoter was present.

Upon closer examination of *aqp-8p::GFP::GCK-3^{WT}* animals, we noticed a striking correlation; 17 out of 21 small adult-like animals showed a weak fluorescence signal above background in other tissues, most notably in the hypodermis (Supplementary Fig. 4B). To test the possibility that the shift of penetrance between the two phenotypic classes may be due to an ectopic expression of GFP::GCK-3^{WT} outside or in addition to the excretory cell, we generated transgenic animals with the hypodermal-specific promoter *dpy-7* (Gilleard et al., 1997). *dpy-7p::GFP::GCK-3^{WT}*-carrying *gck-3(q733)* animals developed in 61% the cases ($n = 51$) into small, small adult-like animals (Figs. 5H, I, and J and Supplementary Fig. 4C). No additional GCK-3 expression beside the hypodermis was observed, suggesting that a hypodermal expression of GCK-3 may be responsible for the increased percentage of small adult-like *aqp-8* transgenic animals. The remaining 39% of *dpy-7p::GFP::GCK-3^{WT}* animals were categorized as L2-like arrested (Fig. 5J). Taken together, we conclude that GCK-3 expression in the hypodermis increases the occurrence of small adult-like animals. The expression of GCK-3 in the excretory cell appears to be unable to rescue any of the two classes of *gck-3(q733)* defective animal types, although it is a major place of GCK-3 expression. Nevertheless, all these transgenic *gck-3(q733)* animals still possess a deformed vulva and seem not to develop into normal-sized adults.

GCK-3 is widely expressed in the adult germ line

A phenotypic trait that surfaced in all our experiments was the strong sterility associated with both classes of *gck-3(q733)* animals or with somatically rescued *let-858p::GFP::GCK-3^{WT}* transgenic *gck-3(q733)* animals. In addition, wild-type oocytes contain *gck-3* mRNA and *gck-3(tm1296)* animals were reported as partially infertile (Denton et al., 2005; Hisamoto et al., 2008). Together, these data suggested that GCK-3 may be expressed in the gonad and, in particular, in germ cells. Hence, we examined the expression and distribution of GCK-3 in the gonad by immunocytochemistry and immunoblotting (Fig. 6).

Extruded gonad preparations of both sexes were immunostained for the presence of GCK-3 (Figs. 6C and D) and PGL-1, a germ cell specific marker that served as a staining and permeability control (data not shown). We found GCK-3 cytoplasmically expressed in essentially all germ cells of both sexes with the exception of mature sperm, where it is not present. In wild-type hermaphrodites, low levels of GCK-3 are visible in mitotic and meiotic germ cells including maturing oocytes (Fig. 6C); this staining is specific as it is much reduced in germ lines of somatically GCK-3^{WT}-rescued animals (data not shown; for oocytes, compare Fig. 6C' with C''). In the male germ line, GCK-3 is upregulated in maturing spermatocytes (compare Fig. 6C with D). Elevated protein levels start to be readily visible in meiotic pachytene and remain high until the secondary spermatocyte stage, at a time when the second meiotic division finishes and GCK-3 is deposited into the residual bodies (Figs. 6C and D). Somatic structures of the gonad also stained specifically with anti-GCK-3 antibodies; an expression of GCK-3 was visible in the distal tip cell and the gonadal sheath cells, including cells of the spermatheca (data not shown).

Next, we evaluated the expression level of gonads compared to the other tissues by probing extracts made from whole worms or gonadal tissue (Figs. 6E and F). In adult hermaphrodites, GCK-3 is expressed to a large extent in the soma, as *glp-1(q224)* mutant worms with

essentially no germ line contain a substantial amount of GCK-3 (Fig. 6E). Males appeared not to contain higher amounts of GCK-3 than hermaphrodites (Fig. 6E). This is in contrast to extracts made from extruded gonads of both sexes where we find that male gonads contain more GCK-3 than hermaphrodite gonads (Fig. 6F). Gonads of somatically GCK-3^{WT}-rescued animals show no detectable endogenous GCK-3 and, therefore, serve as a good specificity control (Fig. 6F). Nevertheless, the GFP::GCK-3 fusion protein is highly expressed, and most of the protein amounts seem to correlate with the strong GFP-fluorescence that we observed in somatic gonadal cells, i.e., sheath cells, spermatheca, and distal tip cell of these animals (data not shown). However, we cannot exclude that the *let-858p* transgene is only partially silenced in germ cells and a small fraction of the GFP::GCK-3 fusion protein is derived from germ cells. In summary, our data demonstrates that endogenous GCK-3 is expressed in the somatic gonad and throughout the germ line, where it accumulates most prominently during spermatogenesis.

GCK-3 has multiple roles in germ line development and is essential for spermatogenesis

Our original *gck-3(RNAi)* experiments suggested germ cell proliferation and differentiation defects. Consistent with the RNAi

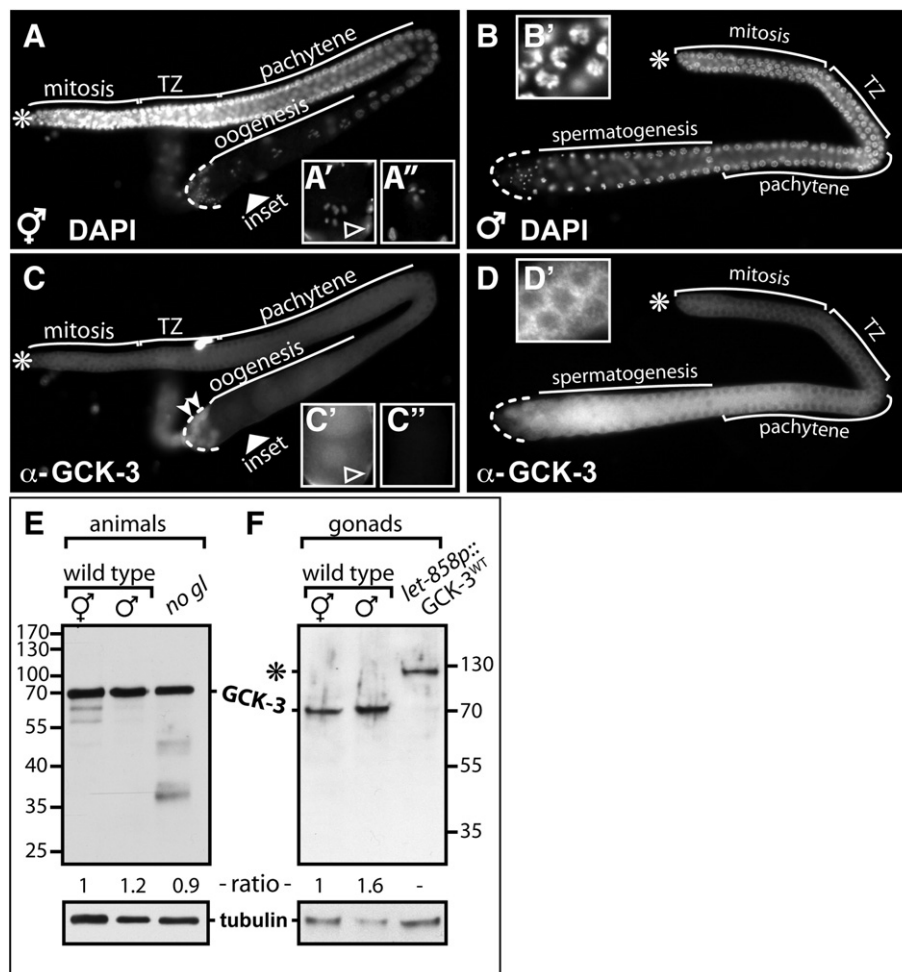


Fig. 6. Germ cell expression of GCK-3 in adult animals. (A–D) Indirect immunocytochemistry of (A and C) hermaphrodite and (B and D) male extruded germ lines. Large arrowhead, regions of panels A and C' insets; Asterisk, distal tip cell. Small arrowheads in panel C point to residual bodies of matured sperm (dashed line). GCK-3 is enriched in the cytoplasm of panels B' and D' germ cells. Note, identical microscopic exposure times and image processing for panels C and D. GCK-3 is expressed in a (C') wild-type but not in a (C'') *gck-3(q733)* oocyte derived from somatic-rescued *gck-3(q733)* hermaphrodites (*let-858p::GCK-3^{WT}*, as shown in Fig. 5B). Comparable exposure times in C' and C'', which are longer than in panels C and D. Empty arrowheads (A', C') point to sheath cells. (E and F) Immunoblots of (E) total worm or (F) extruded germ line (gonad) extracts. Temperature shifted *glp-1(q224)* animals have essentially no germ cells (no gl). Hermaphrodite germ lines from *let-858p::GCK-3^{WT}* serve as a negative control. The asterisk denotes a GFP::GCK-3 translational fusion protein that is predominantly expressed in somatic gonadal cells (see text for details). A quantification of the GCK-3-to-tubulin ratio is given.

results we observed small, underproliferated germ lines lacking mature gametes in *gck-3(q733)* animals (Fig. 3B and Supplementary Figs. 2D and E) and small adult-like *gck-3(q733)* animals, expressing either *aqp-8p::GFP::GCK-3^{WT}* (Supplementary Fig. 4A) or *dpy-7p::GFP::GCK-3^{WT}* (Supplementary Fig. 4C). Occasionally, we detected half-moon shape germ cell nuclei, which are indicative of meiotic entry (Supplementary Fig. 4C). As the overall developmental defects of *gck-3(q733)* animals prevented us from analyzing further germ line development and gametogenesis defects, we turned our attention to the following two strains: the somatic rescued homozygote *gck-3(q733)* background carrying the *let-858p::GFP::GCK-3^{WT}* transgene (referred to as GCK-3^{WT}) animals, and the *gck-3(tm1296)* homozygote progeny from heterozygote mothers.

We find that the majority (86%, $n = 56$) of GCK-3^{WT} animals is sterile and hold no embryos in the uterus. Some animals (14%, $n = 56$) are partially fertile and produced less than 10 dead embryos on average. *gck-3(tm1296)* animals contain on average ~5 embryos ($n = 11$) and produce no living progeny ($n > 100$), suggesting that a reduction of *gck-3* activity in germ cells may cause defective gametogenesis. Similarly, *gck-3(q733)* animals produce no embryos ($n = 137$). To test if the low number of embryos is a consequence of sperm- or oocyte-associated defects, we mated GCK-3^{WT} hermaphrodites with wild-type males; the number of offspring increased to

152 embryos ($n = 14$) with a lethality rate of ~70%. Conversely, *gck-3(tm1296)* males demonstrated poor mating efficiency and rarely managed to produce cross-progeny. These observations suggest that the extremely low number of progeny in *gck-3(q733)* mutants, is a consequence of either a reduced sperm count or of poor quality sperm. Furthermore, there exists a strong maternal contribution of GCK-3 for proper embryogenesis. Unfortunately, we failed to generate GCK-3^{WT} males after many different attempts to test the quality of *gck-3(q733)* sperm directly.

To investigate the likely defects in spermatogenesis more closely, we extruded germ lines from young adult hermaphrodites and adult males (Fig. 7). Characteristic nuclear morphologies, visualized by DAPI staining, allow for the easy identification of each meiotic stage, whereas differentiating sperm cells are also immunoreactive with the antibody SP56 (Figs. 7B–B') (Ward et al., 1986). In wild-type hermaphrodites, each gonad arm contains ~40 immature spermatocytes that progress immediately through both meiotic divisions to produce ~160 mature sperm cells; males produce sperm continuously (Figs. 7A and D).

At first, we noticed that germ lines from GCK-3^{WT} animals vary in size. Although the germ lines of GCK-3^{WT} animals are mostly of similar size compared to wild type, we also found smaller germ lines that appeared under proliferated, which, in extreme cases, were half the

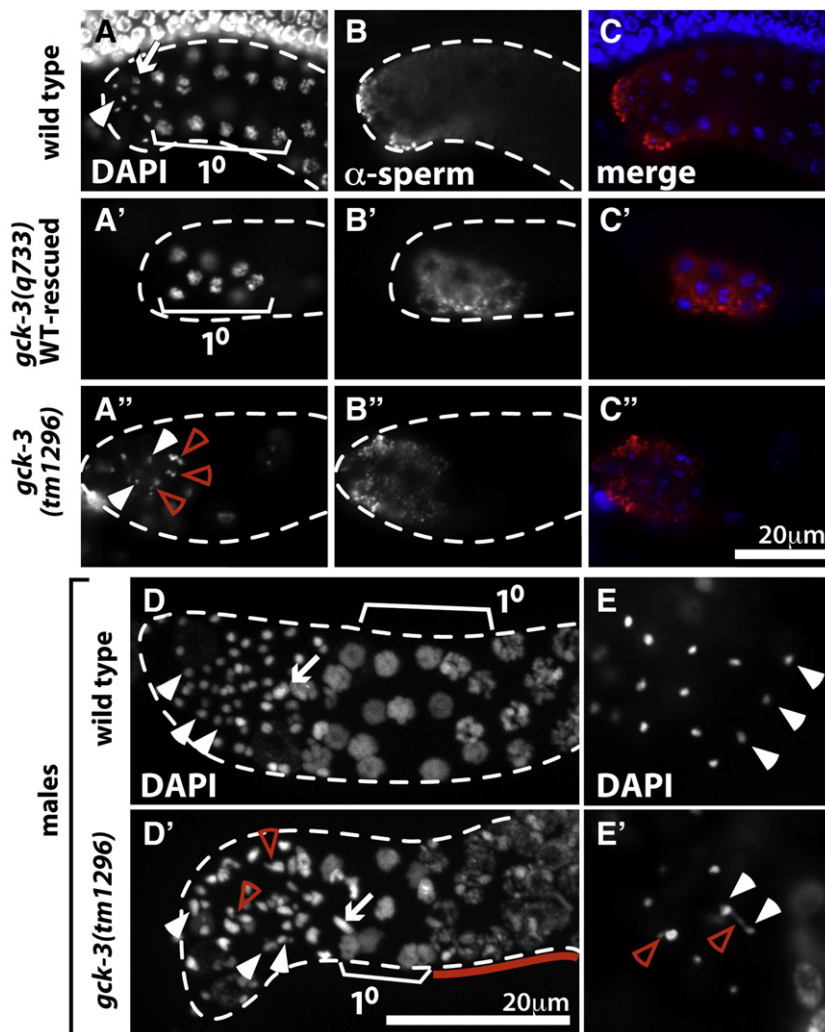


Fig. 7. Spermatogenesis defects in somatic rescued *gck-3* mutant animals. Proximal germ lines (dashed outline) of (A–C'') young adult hermaphrodites and (D'–E') males. Stained with (A, A', A'', D, D', E, E') DAPI and (B, B', B'') the sperm-specific antibody SP56. (C, C', C'') Overlay. (A–C'', E–E') Epifluorescent images. (D, D') Maximum intensity projection images of optical sections. Spermatocytes undergoing the first (1st) and second (arrows) meiotic divisions are outlined; white arrowhead, mature sperm nuclei; red arrowhead, chromatin abnormalities.

size of wild type (data not shown). Similarly, germ lines of *gck-3* (*tm1296*) animals exhibit mild proliferation defects, resulting in smaller germ lines (Supplementary Fig. 2A).

Consistent with the extremely low occurrence of embryos, we find few mature sperm in some GCK-3^{WT} germ lines. Occasionally, we also spotted SP56-positive cells arrested in meiosis II as secondary spermatocytes. For the most part, GCK-3^{WT} animals contain primary spermatocytes arrested in meiosis I (Figs. 7A', B', and C'). The condensed chromatin of these spermatocytes stained also positive for anti-phospho Histone 3, a marker of prometaphase (data not shown). Furthermore, we noticed that mutant germ lines produce on average about 22 ($n=6$) primary spermatocytes, which is an approximately 50% reduction compared to wild type. The observed variability of meiotic defects in somatically rescued animals may reflect an incomplete suppression of the *let-858* promoter in the germ line, and as a consequence, different levels of *gck-3* activities may be required for meiosis. Consistent with this, we also find that hypomorphic *gck-3* (*tm1296*) hermaphrodites contain a larger number of mature sperm (>100). However, their sperm is abnormal as it fails to condense properly and shows signs of chromatin fragmentation (Fig. 7A"). Such morphologically aberrant, mature sperm nuclei are also readily visible in male germ lines (Fig. 7D'). In particular, chromatin bridges connecting condensed sperm nuclei were eminent, suggesting severe chromosome segregation defects (Fig. 7E'). We also noticed that the chromatin of the stages before the first meiotic segregation, i.e., late pachytene and diplotene, was not as condensed and orderly arranged as in wild type (compare Figs. 7D and D').

Taken together, our results clearly demonstrate an involvement of *gck-3* in promoting various steps of overall germ line development. Also, GCK-3 kinase activity is required for the sperm fate and is important for normal progression of male meiosis I and II. The spermatogenesis defects in somatically GCK-3^{WT}-rescued *gck-3*(*q733*) hermaphrodites are severer than those in *gck-3*(*tm1296*) animals. This suggests that the PF2 domain of GCK-3, an established protein interaction domain and presumptive substrate-binding region (Anselmo et al., 2006; Choe and Strange, 2007; Gagnon et al., 2006b; Moriguchi et al., 2005; Piechotta et al., 2003; Vitari et al., 2006), is important for faithful chromosome segregation during meiotic divisions.

Discussion

This study significantly expands the known physiological repertoire of the highly conserved GCK-VI subfamily of Ste20 kinases. GCK-VI kinases are established regulators of ion homeostasis and cell volume control. Our work identified numerous developmental functions in the soma and the germ line for GCK-3, the sole GCK-VI kinase in *C. elegans*. As GCK-VI kinases are extremely well conserved and expressed in a wide variety of tissues, we propose that all members of this Ste20 subfamily may be crucial regulators of a diverse array of likely conserved developmental processes.

The established signaling functions of GCK-3 in osmoregulation

Previous work on GCK-3 supported a conserved role of GCK-VI kinases in ionic stress situations in mammals and *C. elegans*. In the worm, tissue-specific *gck-3* dsRNAi knockdowns in the hypodermis or the intestine, but not in the excretory cell, lead to a failure in acute volume recovery and survival after excessive hypertonic shrinkage, suggesting that the hypodermis and the intestine are organs of osmoregulation and presumed sites of *gck-3* activity (Choe and Strange, 2007). Consistent with this, we also find in our tissue-specific rescue experiments that *gck-3* is active in the hypodermis and contributes to larval progression. If this function is connected to the role of *gck-3* in ion homeostasis is currently unclear, the animals were raised in standard physiological conditions. However, overall expres-

sion in the hypodermis might be low, because we failed to detect a strong hypodermal expression in immunostainings that was above background.

In contrast, we readily observe endogenous GCK-3 expression throughout the entire excretory cell. Recent work by Hisamoto et al. (2008) demonstrated that *gck-3* regulates excretory cell morphology; *gck-3*(*tm1296*) hypomorphic mutants contain excretory canals with shortened posterior ends (Hisamoto et al. 2008). As the *tm1296* mutation is a partial loss of *gck-3* function, we were surprised to find that animals carrying a genetic null mutation in *gck-3* do not display a more drastic shortening of the canals (Fig. 4B). Furthermore, we find that the characteristic morphology of the excretory cell, including its internal organization, appears, to a large extent, similar to wild type (Fig. 3). The canal shortening phenotype was occasionally rescued in animals expressing a fully functional GFP::GCK-3 fusion protein in the excretory cell. Surprisingly, we did not observe a correlation of this partial rescue with the expression levels differences of GFP::GCK-3 amounts. Also, ubiquitously expressing GCK-3^{WT} *gck-3* (*q733*) animals do not have an overt canal shortening defect. This suggests that GCK-3 expression in the excretory cell alone is not sufficient for excretory cell formation, and it is plausible that other tissues may therefore provide *gck-3* function. This hypothesis is consistent with a previous finding that canal defects in *gck-3*(*tm1296*) can be rescued by a heat shock promoter driven GCK-3 expression construct, which is presumably ubiquitously expressed (Hisamoto et al. 2008). Therefore, we propose that *gck-3* activity appears not essential for excretory cell formation *per se* but rather may be required cell autonomously and/or nonautonomously to regulate excretory tube formation, likely as a consequence of its activity in the hypodermis.

C. elegans GCK-3 is placed in a genetic pathway that resembles the signaling pathway of its mammalian orthologs, established in tissue culture (Anselmo et al., 2006; Choe and Strange, 2007; Hisamoto et al., 2008; Moriguchi et al., 2005; Vitari et al., 2006). The only known upstream regulator is WNK-1 kinase, which phosphorylates GCK-3 at position S419 and requires the most C-terminal PF2 domain for its interaction (Hisamoto et al., 2008). GCK-3 uses the same PF2 region for binding to its sole known substrate, the CLC anion channel, CLH-3b (Denton et al., 2005). As GCK-3-mediated phosphorylation of CLH-3b results in channel inhibition (Falin et al., 2009), the down-regulation of *clh-3* activity may suppress *gck-3* mutants. Indeed, a partial rescue of the excretory canal and the fertility defects of the *gck-3*(*tm1296*) hypomorph was reported (Hisamoto et al., 2008). Nevertheless, we were not able to suppress the additional defects of *gck-3*(*q733*) animals with either of the two reported mutant alleles of *clh-3*; e.g., double mutants of *clh-3*(*ok763*);*gck-3*(*q733*) were either L2-like or sterile small adult-like animals. Furthermore, *clh-3* function and CLH-3b expression is only reported for oogenesis (Denton et al., 2005; Rutledge et al., 2001). Taken together, this suggests that the genetic dependency of *gck-3* on *clh-3* activity is most pronounced in the excretory cell and in oocytes. Hence, ion channel regulation may represent only one aspect of the GCK-VI kinase target repertoire.

Novel functions of GCK-3 during postembryonic development

Consistent with a continuous expression throughout development, many tissues were found to require GCK-3 kinase activity during development. However, the expression levels between tissues vary substantially and some tissues are more sensitive to a reduction of *gck-3* activity than others, as demonstrated by dsRNA knockdown experiments or the *tm1296* hypomorph. All known substrates and regulators of GCK-VI kinases require the C-terminal PF2 region (Anselmo et al., 2006; Choe and Strange, 2007; Gagnon et al., 2006b; Moriguchi et al., 2005; Piechotta et al., 2003; Vitari et al., 2006). The PF2 domain is sufficient for all known protein-protein interactions (Choe and Strange, 2007), but this domain is dispensable

for *in vitro* GCK-VI kinase activity (Anselmo et al., 2006; Chen et al., 2004; Gagnon et al., 2006a; Moriguchi et al., 2005). In accordance with this, we find that all somatic functions of GCK-3 require kinase activity, and the phenotypes of animals expressing a C-terminal truncated form of GCK-3 are less severe than the phenotypes of animals with no GCK-3 protein. This suggests that GCK-3 lacking a PF2 domain maintains some kinase activity *in vivo*. Our genetic complementation tests of *gck-3(tm1296)* this interpretation. Furthermore, our comparison of the *gck-3(q733)* phenotypes with transgenic rescuing constructs implies that GCK-3(tm1296) may still be able to recognize some of its substrates, probably through its kinase domain. The identification of these substrates will be a necessary step in the future to understand the many biological roles of GCK-VI kinases.

The complete loss of *gck-3* activity results in a severe derailment of several connected developmental processes, the molting cycle of the animal, and the postembryonic development of the reproductive system. Each molting cycle involves the synthesis of a new cuticle beneath the old one, which is subsequently shed (ecdysis) (Frand et al., 2005). The cuticle represents the worm's exoskeleton and needs to be replaced to allow the growth of the animal to its final adult size. The cuticle is secreted for the most part by the hypodermis. The lateral seam cells generate the alae, which are stage-specific surface modifications of the cuticle (Frand et al., 2005). Our analysis demonstrates that *gck-3* activity is crucial for molting cycles (Fig. 2). L1 larvae require GCK-3 for a timely correct first molting event and subsequently GCK-3 becomes essential for a second molting event, suggesting that different molts may require different *gck-3* activity levels. Furthermore, we speculate that the initial delay may represent a cuticle synthesis problem or may be the consequence of irregular hypodermal development. Interestingly, epithelial expression of GCK-3 with the *dpy-7* promoter increases the percentage of animals that contain adult-type alae on their lateral side although they molted only once. This observation may suggest that in these special non-L2-like cases, the seam cells acquire adult fate and secrete the adult-type alae, while the rest of the hypodermis synthesizes only one postembryonic cuticle. Interestingly, *gck-3(q733)* animals contain a strongly folded intestinal lumen, suggesting that the gut epithelium may continue to grow in size, but the rigid exoskeleton prevents its further expansion. Which endocrine and neuroendocrine pathways are required to trigger epithelial cells to remodel the exoskeleton is still unclear.

The reproduction system of *C. elegans* develops for the most part postembryonically, and its characteristic morphologies are normally used to stage the animal's age. However, loss of *gck-3* activity disrupts the stereotyped and timely coordinated development of the gonad and the vulva; the gonadal and vulval morphologies are reminiscent of the L3 or L4 stage, respectively. Vulva development is initiated by a signal from the gonadal anchor cell (Kimble, 1981; Sulston and White, 1980). The gonadal distal tip cell promotes germ cell proliferation and the U-shaped morphology of the gonad (Kimble and White, 1981). Hence, vulva development in *gck-3(q733)* mutants appears to be a consequence of a correctly specified anchor cell at the L2 stage and the subsequent determination of the vulva precursor cells. However, *gck-3* activity is required at a later stage in the vulva development to go beyond the L4-like vulva morphology. Although this requirement can occasionally be overcome in small adult-like *gck-3(q733)* animals, the everted vulva is abnormal and lacks its normal symmetry, indicating that *gck-3* is important for vulva development at multiple stages. Many signaling cascades are known to be involved in vulva formation, including MAP kinase signaling (reviewed in Sternberg, 2005). As some Ste20 kinases are known to act as upstream regulators of MAPK-mediated signaling (reviewed in Dan et al., 2001), it is tempting to speculate that *gck-3* may regulate vulva development as modulators of MAPK pathways, although alternative possibilities exist. Regardless, the hypodermis and seam cells are together with cells forming the vulva epithelial structures of the worms. Both mammalian

orthologs of GCK-3 are expressed in many epithelial tissues (Chen et al., 2004; Piechotta et al., 2002). Knockout mice for OXSR1 are embryonic lethal and mutants in the *Drosophila* ortholog Fray are larval lethal (Geng et al., 2009; Leiserson et al., 2000). Hence, it is quite conceivable that developmental requirements of GCK-VI kinases and their participation in conserved signaling pathways may also exist in the metazoan phyla, in addition to osmoregulation.

Likely conserved roles for GCK-VI kinases in germ cell development

One newly emerging tissue of overlapping GCK-VI kinase expression and activity is the germ line. Knockout mice of SPAK are only partially fertile and *gck-3(q733)* hermaphrodites are sterile (Geng et al., 2009; Vitari et al., 2005; this study). Germ line development is a multistep process that culminates in the formation of highly differentiated, haploid gametes in adult animals. GCK-3 is expressed continuously throughout female and male germ cell development. Consistent with our finding that GCK-3 abundance peaks during late prophase of male meiosis I, we find *gck-3* activity to be crucial for two aspects of male meiosis: GCK-3 promotes the meiotic progression and ensures proper chromosome segregation. The former phenotype results in the absence of mature sperm and the latter results in aneuploid sperm. As a consequence, hermaphrodites produce little to no offspring, and if so, the embryos arrest in development. Although it is unclear how GCK-3 promotes both meiotic processes, it is obvious that each process is highly sensitive to a reduction of kinase activity or when GCK-3 lacks its PF2 region. Interestingly, mammalian WNK1 is abundantly expressed in testis (Vitari et al., 2005), suggesting that chromosome segregation in male meiosis could be a conserved function of the GCK-VI/WNK pathway. Furthermore, the observed spermatogenesis defects are reminiscent of anaphase promoting complex/cyclosome mutant phenotypes. It is conceivable that the *gck-3/wnk-1* signaling pathway might be involved in this highly conserved cell cycle machinery during meiosis (Golden et al., 2000). Azoospermia, the reduction of a healthy sperm number, is a common cause for a loss in fecundity and may very well be the underlying phenomenon of the reduced litter number of SPAK knockout mice. Further experiments will be required to substantiate this hypothesis.

A truly surprising finding was that *gck-3(q733)* animals fail to develop a robust germ line even in several days old small adult-like mutants. Although germ cells initiated mitotic divisions and produced a larger pool of germ cells, they do not develop any further. As a consequence, the germ line fails to develop its normal meiotic pattern and lacks obvious signs of differentiating gametes. Nevertheless, the germ cells do not overproliferate, suggesting that this is not a simple mitosis-to-meiosis switch defect. Although it is difficult to interpret the germ line defect in the context of the apparent larval arrest, we suggest that low amounts of GCK-3 kinase activity are sufficient to promote meiotic initiation. The level of GCK-3 activity present in *gck-3(tm1296)* animals is sufficient for early meiotic progression. Especially, GCK-3^{WT}-rescued animals display a variety of germ line size defects that range from extremely underproliferated germ lines without gametes, similar to *gck-3(q733)* animals, to almost wild-type-sized germ lines with gametes. This extreme variability is most likely due to a partial silencing of the transgenic array in the germ cells as we were unable to detect the GFP::GCK-3^{WT} protein by direct or indirect immunofluorescence in germ cells. This might suggest that various stages of germ cell development may be sensitive to different levels of *gck-3* activity. In line with this idea is the proposed model that in growing oocytes *gck-3* activity may be diluted to activate the volume-sensitive ion channel CLH-3b (Denton et al., 2005). A dose dependence during meiosis has also been observed for other kinases, such as the classical S-phase kinase CDC7 (Matos et al., 2008) and Aurora-A kinase in *Xenopus* oocyte maturation (Ma et al., 2003). The notion of a possible involvement of GCK-VI kinases in cell cycle progression is

further fueled by the findings of *Drosophila* RNAi screens, where a knockdown of the GCK-VI gene fray in S2 cells causes mitotic spindle defects and abnormal chromosome behavior (Bettencourt-Dias et al., 2004). However, further experiments will be necessary to uncover the molecular details of a likely GCK-VI signaling pathway during meiosis.

This study significantly expands the known physiological repertoire of the highly conserved GCK-VI subfamily of Ste20 kinases. Our analysis of GCK-3 provides a key step to dissect the possible evolutionary conserved signaling pathways that GCK-VI kinases act in during development. Likely cell autonomous and nonautonomous roles of GCK-VI kinases await their discovery.

Acknowledgments

We thank members of the Eckmann laboratory for helpful discussions; Karen Bennett and David Rudel for comments on original versions of the manuscript; the MPI-CBG protein expression, antibody facility and mass spectrometry facility; Jakub Novak and Jana Mäntler for technical help; Judith Kimble for use of the deletion library; Sam Ward for SP56 antibodies, Shohei Mitani (Japanese Knockout Consortium) for *gck-3(tm1296)* and the CGC, which is funded by the NIH, for providing additional worm strains. C.R.E. is an MPI-CBG investigator with financial support for this work provided by the Max Planck Society.

Appendix A. Supplementary data

Supplementary data associated with this article can be found, in the online version, at doi:10.1016/j.ydbio.2010.05.505.

References

- Anselmo, A.N., Earnest, S., Chen, W., Juang, Y.C., Kim, S.C., Zhao, Y., Cobb, M.H., 2006. WNK1 and OSR1 regulate the Na⁺, K⁺, 2Cl⁻ cotransporter in HeLa cells. *Proc. Natl Acad. Sci. USA* 103, 10883–10888.
- Bettencourt-Dias, M., Giet, R., Sinka, R., Mazumdar, A., Lock, W.G., Balloux, F., Zafiroopoulos, P.J., Yamaguchi, S., Winter, S., Carthew, R.W., Cooper, M., Jones, D., Frenz, L., Glover, D.M., 2004. Genome-wide survey of protein kinases required for cell cycle progression. *Nature* 432, 980–987.
- Brenner, S., 1974. The genetics of *Caenorhabditis elegans*. *Genetics* 77, 71–94.
- Chen, W., Yazicioglu, M., Cobb, M.H., 2004. Characterization of OSR1, a member of the mammalian Ste20p/germinal center kinase subfamily. *J. Biol. Chem.* 279, 11129–11136.
- Choe, K.P., Strange, K., 2007. Evolutionarily conserved WNK and Ste20 kinases are essential for acute volume recovery and survival after hypertonic shrinkage in *Caenorhabditis elegans*. *Am. J. Physiol. Cell Physiol.* 293, C915–C927.
- Choi, K.Y., Ji, Y.J., Dhakal, B.K., Yu, J.R., Cho, C., Song, W.K., Ahnm, J., 2003. Vacuolar-type H⁺-ATPase E subunit is required for embryogenesis and yolk transfer in *Caenorhabditis elegans*. *Gene* 311, 13–23.
- Crittenden, S.L., Kimble, J., 1999. Confocal methods for *Caenorhabditis elegans*. *Meth. Mol. Biol.* 122, 141–151.
- Dan, I., Watanabe, N.M., Kusumi, A., 2001. The Ste20 group kinases as regulators of MAP kinase cascades. *Trends Cell Biol.* 11, 220–230.
- Denton, J., Nehrke, K., Yin, X., Morrison, R., Strange, K., 2005. GCK-3, a newly identified Ste20 kinase, binds to and regulates the activity of a cell cycle-dependent CIC anion channel. *J. Gen. Physiol.* 125, 113–125.
- Dowd, B.F., Forbush, B., 2003. PASK (proline-alanine-rich STE20-related kinase), a regulatory kinase of the Na–K–Cl cotransporter (NKCC1). *J. Biol. Chem.* 278, 27347–27353.
- Falin, R.A., Morrison, R., Ham, A.J., Strange, K., 2009. Identification of regulatory phosphorylation sites in a cell volume- and Ste20 kinase-dependent CIC anion channel. *J. Gen. Physiol.* 133, 29–42.
- Frand, A.R., Russel, S., Ruvkun, G., 2005. Functional genomic analysis of *C. elegans* molting. *PLoS Biol.* 3, e312.
- Gagnon, K.B., England, R., Delpire, E., 2006a. Characterization of SPAK and OSR1, regulatory kinases of the Na–K–2Cl cotransporter. *Mol. Cell. Biol.* 26, 689–698.
- Gagnon, K.B., England, R., Delpire, E., 2006b. Volume sensitivity of cation–Cl⁻ cotransporters is modulated by the interaction of two kinases: Ste20-related proline-alanine-rich kinase and WNK4. *Am. J. Physiol. Cell Physiol.* 290, C134–C142.
- Geng, Y., Hoke, A., Delpire, E., 2009. The Ste20 kinases Ste20-related proline-alanine-rich kinase and oxidative-stress response 1 regulate NKCC1 function in sensory neurons. *J. Biol. Chem.* 284, 14020–14028.
- Gilleard, J.S., Barry, J.D., Johnston, I.L., 1997. cis regulatory requirements for hypodermal cell-specific expression of the *Caenorhabditis elegans* cuticle collagen gene *dpy-7*. *Mol. Cell. Biol.* 17, 2301–2311.
- Gobel, V., Barrett, P.L., Hall, D.H., Fleming, J.T., 2004. Lumen morphogenesis in *C. elegans* requires the membrane–cytoskeleton linker erm-1. *Dev. Cell* 6, 865–873.
- Golden, A., Sadler, P.L., Wallenfang, M.R., Schumacher, J.M., Hamill, D.R., Bates, G., Bowerman, B., Seydoux, G., Shakes, D.C., 2000. Metaphase to anaphase (mat) transition-defective mutants in *Caenorhabditis elegans*. *J. Cell Biol.* 151, 1469–1482.
- Hisamoto, N., Moriguchi, T., Urushiyama, S., Mitani, S., Shibuya, H., Matsumoto, K., 2008. *Caenorhabditis elegans* WNK-STE20 pathway regulates tube formation by modulating CIC channel activity. *EMBO Rep.* 9, 70–75.
- Johnston, A.M., Naselli, G., Gonez, L.J., Martin, R.M., Harrison, L.C., DeAizpurua, H.J., 2000. SPAK, a STE20/SPS1-related kinase that activates the p38 pathway. *Oncogene* 19, 4290–4297.
- Junqueira, M., Spirin, V., Santana Balbuena, T., Waridel, P., Surendranath, V., Kryukov, G., Adzhubei, I., Thomas, H., Sunyaev, S., Shevchenko, A., 2008. Separating the wheat from the chaff: unbiased filtering of background tandem mass spectra improves protein identification. *J. Proteome Res.* 7, 3382–3395.
- Kelly, W.G., Xu, S., Montgomery, M.K., Fire, A., 1997. Distinct requirements for somatic and germline expression of a generally expressed *Caenorhabditis elegans* gene. *Genetics* 146, 227–238.
- Kimble, J., 1981. Alterations in cell lineage following laser ablation of cells in the somatic gonad of *Caenorhabditis elegans*. *Dev. Biol.* 87, 286–300.
- Kimble, J., Hirsh, D., 1979. The postembryonic cell lineages of the hermaphrodite and male gonads in *Caenorhabditis elegans*. *Dev. Biol.* 70, 396–417.
- Kimble, J.E., White, J.C., 1981. On the control of germ cell development in *Caenorhabditis elegans*. *Dev. Biol.* 81, 208–219.
- Kraemer, B., Crittenden, S., Gallegos, M., Moulder, G., Barstead, R., Kimble, J., Wickens, M., 1999. NANOS-3 and FBF proteins physically interact to control the sperm-oocyte switch in *Caenorhabditis elegans*. *Curr. Biol.* 9, 1009–1018.
- Lee, B.H., Min, X., Heise, C.J., Xu, B.E., Chen, S., Shu, H., Luby-Phelps, K., Goldsmith, E.J., Cobb, M.H., 2004. WNK1 phosphorylates synaptotagmin 2 and modulates its membrane binding. *Mol. Cell* 15, 741–751.
- Leiserson, W.M., Harkins, E.W., Keshishian, H., 2000. Fray, a *Drosophila* serine/threonine kinase homologous to mammalian PASK, is required for axonal ensheathment. *Neuron* 28, 793–806.
- Ma, C., Cummings, C., Liu, X.J., 2003. Biphasic activation of Aurora-A kinase during the meiosis I–meiosis II transition in *Xenopus* oocytes. *Mol. Cell. Biol.* 23, 1703–1716.
- Mah, A.K., Armstrong, K.R., Chew, D.S., Chu, J.S., Tu, D.K., Johnsen, R.C., Chen, N., Chamberlin, H.M., Baillie, D.L., 2007. Transcriptional regulation of AQP-8, a *Caenorhabditis elegans* aquaporin exclusively expressed in the excretory system, by the POU homeobox transcription factor CEH-6. *J. Biol. Chem.* 282, 28074–28086.
- Manning, G., 2005. Genomic overview of protein kinases. In: T. C. e. R. Community, (Ed.), *WormBook*. WormBook, 2005.
- Matos, J., Lipp, J.J., Bogdanova, A., Guillot, S., Okaz, E., Junqueira, M., Shevchenko, A., Zachariae, W., 2008. Dbf4-dependent CDC7 kinase links DNA replication to the segregation of homologous chromosomes in meiosis I. *Cell* 135, 662–678.
- McDonald, K.L., Mophew, M., Verkade, P., Muller-Reichert, T., 2007. Recent advances in high-pressure freezing: equipment- and specimen-loading methods. *Meth. Mol. Biol.* 369, 143–173.
- Miller, D.M., Shakes, D.C., 1995. Immunofluorescence microscopy. *Meth. Cell Biol.* 48, 365–394.
- Moriguchi, T., Urushiyama, S., Hisamoto, N., Iemura, S., Uchida, S., Natsume, T., Matsumoto, K., Shibuya, H., 2005. WNK1 regulates phosphorylation of cation–chloride-coupled cotransporters via the STE20-related kinases, SPAK and OSR1. *J. Biol. Chem.* 280, 42685–42693.
- Muller-Reichert, T., Hohenberg, H., O'Toole, E.T., McDonald, K., 2003. Cryoimmobilization and three-dimensional visualization of *C. elegans* ultrastructure. *J. Microsc.* 212, 71–80.
- Nelson, F.K., Riddle, D.L., 1984. Functional study of the *Caenorhabditis elegans* secretory–excretory system using laser microsurgery. *J. Exp. Zool.* 231, 45–56.
- Oh, E., Heise, C.J., English, J.M., Cobb, M.H., Thurmond, D.C., 2007. WNK1 is a novel regulator of Munc18c–Syntaxin 4 complex formation in soluble NSF attachment protein receptor (SNARE)-mediated vesicle exocytosis. *J. Biol. Chem.* 282, 32613–32622.
- Peters, A.H., Kubicek, S., Mechtler, K., O'Sullivan, R.J., Derijck, A.A., Perez-Burgos, L., Kohlmaier, A., Opravil, S., Tachibana, M., Shinkai, Y., Martens, J.H., Jenuwein, T., 2003. Partitioning and plasticity of repressive histone methylation states in mammalian chromatin. *Mol. Cell* 12, 1577–1589.
- Piechotta, K., Lu, J., Delpire, E., 2002. Cation chloride cotransporters interact with the stress-related kinases Ste20-related proline-alanine-rich kinase (SPAK) and oxidative stress response 1 (OSR1). *J. Biol. Chem.* 277, 50812–50819.
- Piechotta, K., Garbarini, N., England, R., Delpire, E., 2003. Characterization of the interaction of the stress kinase SPAK with the Na⁺–K⁺–2Cl⁻ cotransporter in the nervous system: evidence for a scaffolding role of the kinase. *J. Biol. Chem.* 278, 52848–52856.
- Riddle, D.L., Swanson, M.M., Albert, P.S., 1981. Interacting genes in nematode dauer larva formation. *Nature* 290, 668–671.
- Rutledge, E., Bianchi, L., Christensen, M., Boehmer, C., Morrison, R., Broslat, A., Beld, A.M., George, A.L., Greenstein, D., Strange, K., 2001. CLH-3, a CIC-2 anion channel ortholog activated during meiotic maturation in *C. elegans* oocytes. *Curr. Biol.* 11, 161–170.
- Shevchenko, A., Tomas, H., Havlis, J., Olsen, J.V., Mann, M., 2006. In-gel digestion for mass spectrometric characterization of proteins and proteomes. *Nat. Protoc.* 1, 2856–2860.
- Sternberg, P.W., 2005. Vulval development. *WormBook*, pp. 1–28.
- Strange, K., Denton, J., Nehrke, K., 2006. Ste20-type kinases: evolutionarily conserved regulators of ion transport and cell volume. *Physiol. (Bethesda)* 21, 61–68.
- Sulston, J.E., Horvitz, H.R., 1977. Post-embryonic cell lineages of the nematode, *Caenorhabditis elegans*. *Dev. Biol.* 56, 110–156.

- Sulston, J.E., White, J.G., 1980. Regulation and cell autonomy during postembryonic development of *Caenorhabditis elegans*. *Dev. Biol.* 78, 577–597.
- Vitari, A.C., Deak, M., Morrice, N.A., Alessi, D.R., 2005. The WNK1 and WNK4 protein kinases that are mutated in Gordon's hypertension syndrome phosphorylate and activate SPAK and OSR1 protein kinases. *Biochem. J.* 391, 17–24.
- Vitari, A.C., Thastrup, J., Rafiqi, F.H., Deak, M., Morrice, N.A., Karlsson, H.K., Alessi, D.R., 2006. Functional interactions of the SPAK/OSR1 kinases with their upstream activator WNK1 and downstream substrate NKCC1. *Biochem. J.* 397, 223–231.
- Ward, S., Roberts, T.M., Strome, S., Pavalko, F.M., Hogan, E., 1986. Monoclonal antibodies that recognize a polypeptide antigenic determinant shared by multiple *Caenorhabditis elegans* sperm-specific proteins. *J. Cell Biol.* 102, 1778–1786.
- Xu, B., English, J.M., Wilsbacher, J.L., Stippec, S., Goldsmith, E.J., Cobb, M.H., 2000. WNK1, a novel mammalian serine/threonine protein kinase lacking the catalytic lysine in subdomain II. *J. Biol. Chem.* 275, 16795–16801.
- Xu, B.E., Stippec, S., Lenertz, L., Lee, B.H., Zhang, W., Lee, Y.K., Cobb, M.H., 2004. WNK1 activates ERK5 by an MEKK2/3-dependent mechanism. *J. Biol. Chem.* 279, 7826–7831.
- Zagorska, A., Pozo-Guisado, E., Boudeau, J., Vitari, A.C., Rafiqi, F.H., Thastrup, J., Deak, M., Campbell, D.G., Morrice, N.A., Prescott, A.R., Alessi, D.R., 2007. Regulation of activity and localization of the WNK1 protein kinase by hyperosmotic stress. *J. Cell Biol.* 176, 89–100.
- Zambrowicz, B.P., Abuin, A., Ramirez-Solis, R., Richter, L.J., Piggott, J., BeltrandelRio, H., Buxton, E.C., Edwards, J., Finch, R.A., Friddle, C.J., Gupta, A., Hansen, G., Hu, Y., Huang, W., Jaing, C., Key Jr., B.W., Kipp, P., Kohlhauff, B., Ma, Z.Q., Markesich, D., Payne, R., Potter, D.G., Qian, N., Shaw, J., Schrick, J., Shi, Z.Z., Sparks, M.J., Van Sligtenhorst, I., Vogel, P., Walke, W., Xu, N., Zhu, Q., Person, C., Sands, A.T., 2003. Wnk1 kinase deficiency lowers blood pressure in mice: a gene-trap screen to identify potential targets for therapeutic intervention. *Proc. Natl Acad. Sci. USA* 100, 14109–14114.